Applied Physics Letters

Experimental demonstration of elastic analogues of nonseparable qutrits

Cite as: Appl. Phys. Lett. **116**, 164104 (2020); https://doi.org/10.1063/1.5145097
Submitted: 14 January 2020 . Accepted: 07 April 2020 . Published Online: 24 April 2020

M. Arif Hasan, Lazaro Calderin, Trevor Lata, Pierre Lucas, Keith Runge, and Pierre A. Deymier

AIP Publishing

Experimental demonstration of elastic analogues of nonseparable qutrits

Cite as: Appl. Phys. Lett. **116**, 164104 (2020); doi: 10.1063/1.5145097
Submitted: 14 January 2020 · Accepted: 7 April 2020 ·
Published Online: 24 April 2020

View Online Export Citation CrossMark

M. Arif Hasan,[a)] Lazaro Calderin,[b)] Trevor Lata,[b)] Pierre Lucas,[b)] Keith Runge,[b)] and Pierre A. Deymier[b)]

AFFILIATIONS

Department of Materials Science and Engineering, University of Arizona, Tucson, Arizona 85721, USA

[a)]Author to whom correspondence should be addressed: mdhasan@email.arizona.edu
[b)]Electronic addresses: lcalderin@email.arizona.edu; tlata157@email.arizona.edu; pierre@email.arizona.edu; krunge@email.arizona.edu; and deymier@email.arizona.edu

ABSTRACT

The creation of multilevel quantum states, qudits, has revolutionized concepts for quantum computing. Classical systems that capture behavior analogous to quantum systems have been demonstrated. In this spirit, we consider a three-level classical analogue of the qudit composed of coupled acoustic waveguides. Here, we demonstrate both the experimental realization of a three-level classical analogue of the qudit and the creation and tuning of nonseparable superpositions of two of these analogues, which are classically "entangled." Measurements of velocities and transmission inform our assignment of these nonseparable states.

Quantum information processing paradigms promise a new era in computational power as illustrated by recent advances.[1] The quantum bit (qubit), which is a critical component of all quantum computing platforms, is currently based on quantum particles or quantum systems that are extremely sensitive to environmental conditions and lose their superposition of states by decoherence. Coherence times can be increased by operating at cryogenic temperature. Furthermore, the measurement on quantum systems in the superposition of states leads to collapse of the wave function onto pure states, requiring the use of statistical approaches should the original superposition needs to be reconstructed. To overcome these critical drawbacks, we theoretically proposed[2,3] and experimentally realized[4] the concept of a one-dimensional (1D) elastic pseudospin, which we call a phi-bit. The concept of pseudospin has also been explored in various other topological systems.[5–15] An elastic phi-bit exhibits pseudospin characteristics, i.e., coherent superposition of states in the directions of propagation. The elastic pseudospin superposition of states are stable at room temperature and decoherence free. It is measurable without wave function collapse as it represents an actual amplitude and not a probability amplitude.

Quantum entanglement is an essential ingredient for applications of quantum information processing.[16] The creation of a large number of entangled qubits is needed for measurement-based quantum computation,[17] quantum simulation,[18] and quantum error correction.[19,20] One of the experimental challenges in creating and engineering entanglement of multiple qubits[21–23] is noise control,[24] and scaling up is difficult due to decoherence. Quantum entangled systems exhibit nonseparability, which is important for quantum computing applications and may be achieved classically.[25] Classical "entanglement," i.e., a local nonseparable superposition of states,[26] has been discussed in great detail in the field of optics[27–36] and, recently, in acoustics[37–40] and has found applications in quantum information science.[41–43]

A multiple phi-bit system can be constructed as a system of elastically coupled 1D waveguides. The amplitude in the different waveguides is analogous to an orbital angular momentum (OAM) degrees of freedom,[37,38] and the amplitude of the pseudospin elastic waves takes the form of a spinor in the two-dimensional Hilbert space of the direction of propagation along the waveguides. Recently, we experimentally demonstrated the existence of elastic waves that are nonseparable linear combinations of tensor product states of two pseudospin and two OAM degrees of freedom.[39] These states lie in the tensor product Hilbert space of the two-dimensional subspaces associated with the direction of propagation and OAM. This elastic system is, therefore, analogous to a two-partite two-level quantum system. Nonetheless, the total dimensionality of Hilbert space can, in principle, be increased by considering multilevel systems of qubits or phi-bits. The possibility of using multilevel systems has led to growing interest in the enhancement of entanglement in higher dimensions, i.e., multidimensional Hilbert space.[44–56] One such example is a qudit with a d-level quantum system, and a three-level qutrit is achieved when $d = 3$. Such high-dimensional entangled states have been realized with biphotons[57] or nitrogen-vacancy centers in diamond.[58–60] In contrast, no attention has been paid to the high-dimensional nonseparable states of elastic waves. In this Letter, we propose and demonstrate the concept of a phi-trit, which is a 1D elastic system that can support a superposition of three mutually orthogonal elastic states. Furthermore, we experimentally demonstrate the preparation and tunability of acoustic nonseparable states of two phi-trits.

The phi-trit is realized as an elastic system composed of a parallel array of four identical 1D waveguides coupled elastically along their length. Let us define $u_{4\times1}$ a vector whose components, $u_i,\ i = 1,\ldots,4$, represent the displacement of the *i*th waveguide (see the supplementary material, Note 1). For plane wave displacements, $u_i = A_i e^{ikx} e^{i\omega t}$, where A_i are the amplitudes and k and ω are the wave number and angular frequency; the dispersion relation is $\omega_{j,k}^2 = (\beta k)^2 + \lambda_j \eta^2$; $j = 1, 2, \ldots, 4$. The set of amplitudes in the waveguides, A_i, is analogous to OAM degrees of freedom. The parameter β is proportional to the speed of sound in the waveguides, and η measures the strength of the elastic coupling between waveguides. λ_j are the eigenvalues associated with the given OAM eigenmode $|j\rangle_{OAM}$. The dispersion relations with cutoff frequencies represent the states that are coherent superpositions of elastic waves propagating in opposite directions along the waveguides, analogous to a superposition of spin states (thus, the name pseudospin).[4] At $k = 0$, the elastic wave is standing and the amplitudes in the two opposite directions are equal. For large positive or negative k, a single direction dominates. k is a good number to characterize the state of the elastic waves in the space of directions of propagation. These elastic waves are analogous to a two-partite system identified by the OAM and pseudospin degrees of freedom, and the latter are labeled by the wave number k. Moreover, in the four waveguide system, the OAM has three mutually orthogonal elastic states $|2\rangle_{\mathrm{OAM}}, |3\rangle_{\mathrm{OAM}}, \mathit{and}\ |4\rangle_{\mathrm{OAM}}$, thus realizing one phi-trit. The wave number k has, in principle, an infinite number of orthogonal states. In a finite length waveguide, the wave number space is discrete, and we can select and represent three pseudospin states with the labels $|k_2\rangle, |k_3\rangle, \mathit{and}|k_4\rangle$ associated with the corresponding wave numbers to realize a second phi-trit. A general state of the system is then written as

$$u_{4\times1} = \sum_{j,l} A_{j,l} |j\rangle_{OAM} \otimes |k_l\rangle\, e^{i\omega_l t}. \tag{1}$$

By choosing a particular frequency ω for exciting the system, we create a superposition of these mutually orthogonal elastic states (i.e., Bell states) in the generally nonseparable phi-trit,

$$u_{4\times1} = \left(A_{2,2}|2\rangle_{OAM}\otimes|k_2\rangle + A_{3,3}|3\rangle_{OAM}\otimes|k_3\rangle + A_{4,4}|4\rangle_{OAM}\otimes|k_4\rangle\right)e^{i\omega t}. \tag{2}$$

The Bell state coefficients $A_{2,2},\ A_{3,3}, \mathit{and}\ A_{4,4}$ are complex amplitudes,[39] which can be controlled in experiment. In Eq. (2), we have constructed a superposition of isofrequency states ($\omega_2 = \omega_3 = \omega_4 = \omega$), which is nonseparable except for certain choices of $A_{2,2}, A_{3,3}, \mathit{and}\ A_{4,4}$. The wave numbers $k_2,\ k_3, \mathit{and}\ k_4$ correspond to the modes in the three OAM bands $|2\rangle_{OAM}, |3\rangle_{OAM}, \mathit{and}\ |4\rangle_{OAM}$ with the same frequency ω. In this superposition, both the eigenvectors of the OAM degree of freedom and the wave numbers are different. For most $A_{2,2},\ A_{3,3}, \mathit{and}\ A_{4,4}$, this superposition of states cannot be written in the form of a tensor product of OAM eigenvectors and pseudospin states.

The experimental realization of nonseparable phi-trits consists of four elastically coupled aluminum rods (waveguides). We employ ultrasonic spectroscopy techniques to characterize the states of this system (the details of the experimental system are outlined in the supplementary material, Note 2). The experiment is carried out by first stimulating the coupled waveguides with each of the OAM eigenvectors, $|j\rangle_{OAM}; j = 1,\ldots,4$, at one end of the rods, and collecting the transmission recorded by transducers at the other end of the rods. Figure 1(a) shows the measured experimental transmission spectra. The $|2\rangle_{OAM}, |3\rangle_{OAM}, \mathit{and}\, |4\rangle_{OAM}$ OAM modes show a significant depression in the transmission amplitude below a cutoff frequency, and well-defined resonances are spaced more closely near the cutoff. These resonances correspond to the standing-wave modes supported by the finite waveguide and can be associated with pseudospin states. To calculate the wavelength corresponding to the standing-wave modes, we use a full-field scanning laser vibrometer (PSV-400). We measure the velocity field along the length of the first rod in the transverse direction, which maps the elastic field of longitudinal modes. Figures 1(b) and 1(c) show laser vibrometer measurements showing the mode shapes of $|2\rangle_{OAM}$ at 28.8 kHz and $|4\rangle_{OAM}$ at 56.6 kHz. Two snapshots of the spatial waveforms are reported for time t_1 and t_2, showing seven nodes for $|2\rangle_{OAM}$ and 12 nodes for $|4\rangle_{OAM}$. Hence, the wavelength corresponding to the standing waves can be easily determined from the expression $\lambda = 2L/n$; n is an integer corresponding to the number of nodes of the standing waves. A wave number can subsequently be calculated as $k = 1/\lambda$. From the experimentally

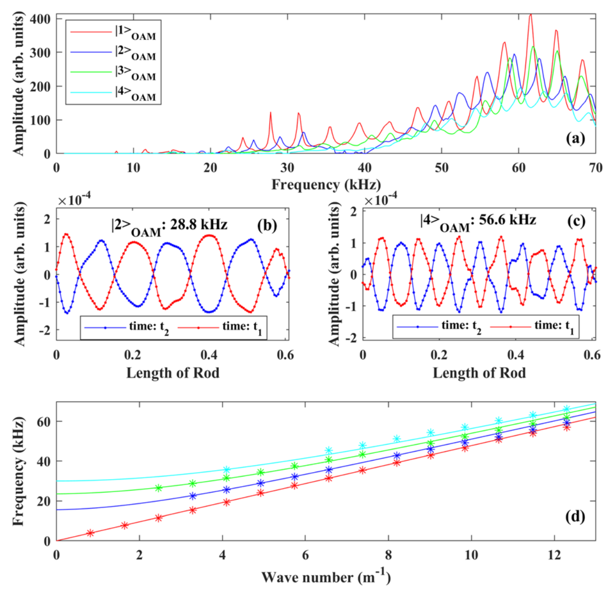

FIG. 1. (a) Transmission spectrum of the coupled four-rod waveguides for the four OAM eigenmodes of $|1\rangle_{OAM}, |2\rangle_{OAM}, |3\rangle_{OAM}, \mathit{and}\, |4\rangle_{OAM}$. The transmission amplitude is in arbitrary units. (b) and (c) Velocity field along the length of the first rod in the transverse direction that maps the elastic field of longitudinal modes of branch $|2\rangle_{OAM}$ at 28.8 kHz and $|4\rangle_{OAM}$ at 56.6 kHz. Two snapshots of the spatial waveforms are reported for times t_1 and t_2, showing seven nodes for $|2\rangle_{OAM}$ and 12 nodes for $|4\rangle_{OAM}$. (d) Band structure determined and calculated from (a)–(c). The asterisks in (d) are obtained from the experimentally identifiable resonances of (a), and the solid lines associated with the asterisks are a fit to these identifiable resonances using the dispersion relation.

identifiable resonant frequency $(\omega_{j,k})$ and the associated wave number, we obtain the dispersion relation of the second, third, and fourth bands that possess pseudospin character[4] with cutoff frequencies $|2\rangle_{OAM}$: 15.53 kHz, $|3\rangle_{OAM}$: 23.52 kHz, and $|4\rangle_{OAM}$: 30.00 kHz.

The resonances shown in Fig. 1 correspond to separable states, i.e., states expressible as tensor products of OAM and pseudospin degrees of freedom. The OAM degree of freedom has three possible values. By limiting the pseudospin degree of freedom to three possible wave numbers or linear combinations of wave numbers, we can create a nonseparable superposition of states of this two-partite three-level elastic system. Such a superposition of isofrequency elastic states of the coupled rod system corresponds to the linear combination of products of the three nonzero OAM eigenstates and the corresponding pseudospin states, as shown in Eq. (1). From Fig. 1(a), we identify the isofrequency, $\omega_I = 56.6$ kHz, at which there is substantial transmissions of three OAM eigenvectors $|2\rangle_{OAM}, |3\rangle_{OAM}, \textit{and}\, |4\rangle_{OAM}$. To excite such a nonseparable superposition of states experimentally, the coupled elastic system is driven with the external force $\vec{F}e^{i\omega_I t}; \vec{F} = \left(\sqrt{1-\alpha^2-\beta^2}\right)|4\rangle_{OAM} + \alpha|3\rangle_{OAM} + \beta|2\rangle_{OAM}, \beta = \sqrt{1-\alpha^2}\sin(\alpha\pi)$. Moreover, by tuning the parameter α, the contribution of the three linear combinations of eigenmode vibrations $(|2\rangle_{OAM}, |3\rangle_{OAM}, \textit{and}\, |4\rangle_{OAM})$ are experimentally manipulated. Figure 2(a) shows the phase difference (ϕ_{ij}) between the transmissions for each pair of rods as a function of α, where $\phi_{ij} = \frac{180}{\pi}\cos^{-1}\left(\frac{i.j}{|i||j|}\right); i,j = 1,\ldots,4$. For a pure eigenmode, the phase difference between the transmissions for each pair of rods is $\phi_{12}^{|2\rangle_{OAM}} = \phi_{34}^{|2\rangle_{OAM}} = 0$ and $\phi_{23}^{|2\rangle_{OAM}} = 180^o$ for $|2\rangle_{OAM}$, $\phi_{12}^{|3\rangle_{OAM}} = \phi_{34}^{|3\rangle_{OAM}} = 180^o$ and $\phi_{23}^{|3\rangle_{OAM}} = 0$ for $|3\rangle_{OAM}$, and $\phi_{12}^{|4\rangle_{OAM}} = \phi_{23}^{|4\rangle_{OAM}} = \phi_{34}^{|4\rangle_{OAM}} = 180^o$ for $|4\rangle_{OAM}$. From Fig. 2(a), we indeed see that manipulation of the parameter α can be used to tune the superposition: (i) for $\alpha = 0$, the output mode of vibration is almost purely $|4\rangle_{OAM}$ since $\phi_{12}^{|4\rangle_{OAM}}, \phi_{23}^{|4\rangle_{OAM}}$, and $\phi_{34}^{|4\rangle_{OAM}}$ are close to 180 degree; (ii) for $\alpha = 1$, the vibrational mode is almost purely $|3\rangle_{OAM}$; (iii) for $\alpha = 0.5$, the driving force becomes $\vec{F} = |3\rangle_{OAM}/2 + \sqrt{3}|4\rangle_{OAM}/2$, which leads to a nonseparable superposition of isofrequency states in the bands corresponding to the two OAM eigenvectors $|2\rangle_{OAM}$ and $|3\rangle_{OAM}$;[39] and finally, (iv) for any other α value, the output is a linear combination of the tensor product of OAM eigenmodes of $|2\rangle_{OAM}, |3\rangle_{OAM}, \textit{and} |4\rangle_{OAM}$ with the corresponding k-labeled pseudospin, i.e., the state of two nonseparable phi-trits [Eq. (2)]. Such a nonseparable state of phi-trits is analogous to a "classically entangled" two-partite three-level quantum system.

We also show the eigenmode superposition in terms of pseudospin states of the elastic waves, i.e., the wave number k. The experimental conditions of Fig. 1(a) enable us to resolve resonances with frequencies close to the cutoff frequency, giving exquisite control on the elastic pseudospins. To experimentally map the pseudospin states for the isofrequency value of $\omega_I = 56.6$ kHz, we choose five different α values , $\alpha = 0$, 0.25, 0.50, 0.75, 1.0. As before, by means of laser vibrometry, we map the longitudinal mode elastic field for each of the α values. Moreover, to have a better resolution in the spatial waveform, especially for high frequency value of $\omega_I = 56.6$ kHz, we choose a total of 257 laser incident points along the length of the rod. From the spatial waveform, we then calculate the wave number associated with each mode of oscillation by using a Fourier transform in space. Due to

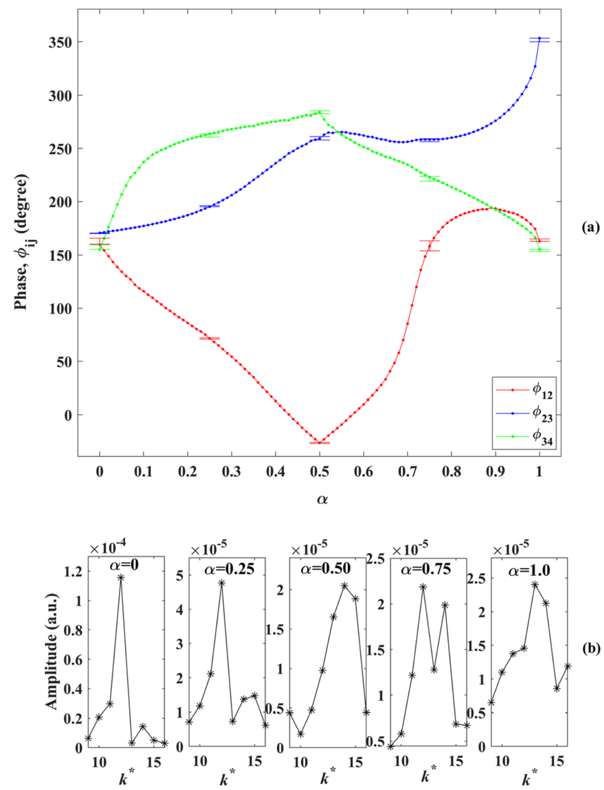

FIG. 2. Creation of nonseparable states of two phi-trits by the external driving force $\vec{F}e^{i\omega_I t}; \vec{F} = \left(\sqrt{1-\alpha^2-\beta^2}\right)|4\rangle_{OAM} + \alpha|3\rangle_{OAM} + \beta|2\rangle_{OAM}$, $\beta = \sqrt{1-\alpha^2}\sin(\alpha\pi)$, and driving frequency $\omega_I = 56.6$ kHz. (a) Variations of the phase differences (ϕ_{ij}) between pairs of rods of the coupled waveguides as a function of α; to better visualize the plot, the error bars are shown only for $\alpha = 0$, 0.25, 0.5, 0.75, 1.0. (b) Spatial Fourier transform, revealing the wave numbers, and hence the superposition of states associated with different α values: (i) for $\alpha = 0$, the output vibrational mode is almost purely $|4\rangle_{OAM}$; (ii) for $\alpha = 1$, the vibrational mode is almost purely $|3\rangle_{OAM}$; (iii) for $\alpha = 0.5$, we have the nonseparable superposition of isofrequency states in the bands corresponding to the two OAM eigenvectors $|2\rangle_{OAM}$ and $|3\rangle_{OAM}$; and finally, (iv) for $\alpha = 0.25$ and 0.75, the vibrational mode is a linear combinations of OAM eigenmodes of $|2\rangle_{OAM}, |3\rangle_{OAM}$, and $|4\rangle_{OAM}$, i.e., two nonseparable phi-trits.

their finite length, the rods only support standing waves; we assume that the wavelengths are multiples of $2L$, i.e., $k^* = k(2L)$ is an integer. Figure 2(b) shows the variations of the wave number that maps various pseudospin states as we move from $\alpha = 0$ to 1. For the nearly pure eigenmode of oscillation $|4\rangle_{OAM}$ at $\alpha = 0$, it is clear that $k^* = 12$ has the highest amplitude, and for $|3\rangle_{OAM}$, at $\alpha = 1$, the highest amplitude is at $k^* = 13$. These two states are separable states, namely , $|4\rangle_{OAM} \otimes |k_4^* = 12\rangle$ and $|3\rangle_{OAM} \otimes |k_3^* = 13\rangle$. When $\alpha = 0.5$, Fig. 2(b) shows that the amplitude of $k^* = 12$ is small in comparison to the amplitudes of $k^* = 13$, 14, and 15, which are the wavenumbers for $|2\rangle_{OAM}$ and $|3\rangle_{OAM}$ states [cf. Fig. 1(b)]. Therefore, the third term in Eq. (2) has a negligible amplitude. The wavenumbers of the states with the largest amplitudes along the two bands with cutoff frequencies $(|2\rangle_{OAM}$ and $|3\rangle_{OAM})$ are $k_2^* = 14$, $k_2^{*\prime} = 15$, and $k_3^* = 13$. The first term of Eq. (2) can be written as the superposition of two states k_2^* and $k_2^{*\prime}$ with OAM eigenvector $|2\rangle_{OAM}$ and frequency ω_I that contribute the largest amplitudes, namely, $A_{2,2} = A_{2,2}(k_2^*)$ *and* $A_{2,2'} = A_{2,2}(k_2^{*\prime})$. Equation (2) reduces to $u_{4\times1} = (A_{2,2}|2\rangle_{OAM} \otimes |k_2^*\rangle + A_{2,2'}|2\rangle_{OAM} \otimes|k_2^{*\prime}\rangle + A_{3,3}|3\rangle_{OAM} \otimes |k_3{}^*\rangle)\, e^{i\omega_I t}$. Hence, $\alpha = 0.5$ corresponds to a nonseparable superposition of isofrequency states in the bands corresponding to the two OAM eigenvectors $|2\rangle_{OAM}$ and $|3\rangle_{OAM}$ and pseudospin states.[39] Finally, for $\alpha = 0.25$ and 0.75, we have a nonseparable superposition of isofrequency states in the bands corresponding to the three OAM eigenvectors and the corresponding pseudospin states, i.e., we have realized two nonseparable phi-trits. In particular, for $\alpha = 0.75$, we see that the amplitudes corresponding to $k^* = 11, 12, 13, \text{and}\ 14$ are the highest, a clear signature of two nonseparable phi-trits. For such a case, Eq. (2) takes the form $u_{4\times1} = (A_{2,2}|2\rangle_{OAM} \otimes |k_2^*\rangle + A_{3,3}|3\rangle_{OAM} \otimes |k_3{}^*\rangle + A_{4,4}|4\rangle_{OAM} \otimes |k_4^*\rangle + A_{4,4'}|4\rangle_{OAM} \otimes |k_4^{*\prime}\rangle)\, e^{i\omega_I t}$. Note that the kets of differing waves are orthogonal.

We now calculate the entropy of classical entanglement, to quantify the level of nonseparability. To do so, first, we determine the Bell state complex coefficients for different values of $\alpha = 0$, 0.5, 0.75, 1.0 (see the supplementary material, Note 3). We then calculate the entropy of entanglement,[61] S, for the two nonseparable states corresponding to (i) $\alpha = 0.5$, and (ii) $\alpha = 0.75$. Using our experimental measurements, we find (i) $S^{(i)} = 0.84 ln2 \pm 0.01 ln2$, which is only about 16% less than $ln2$, the entropy of two phi-bits maximally entangled, and (ii) $S^{(ii)} = 0.95 ln3 \pm 0.02 ln3$, which is only about 5% less than $ln3$, the entropy of two phi-trits maximally entangled (see the supplementary material, Note 3).

We have experimentally demonstrated the existence and manipulation of the nonseparable superposition of states in an elastic system composed of two subsystems, each supporting three states. Each subsystem acts as an elastic analogue of a qutrit, called a phi-trit. The first phi-trit is associated with the OAM degrees of freedom of a parallel array of four coupled elastic waveguides. The second one is associated with the direction of propagation degrees of freedom along the waveguides. The amplitude of the superposition is complex, i.e., supports a phase. Therefore, this work offers an innovative direction for realizing and manipulating the coherent nonseparable superposition of elastic states that are analogous to quantum states without their drawback. The experimental demonstration of our entangled states realizes the potential of acoustic waves to capture phenomena previously associated with optics. Recently, the use of classical light with entangled degrees of freedom has found applications in quantum information[62] and metrology.[42,63] Our works suggest that the same sort of applications can be realized with acoustic systems. In electromagnetic systems, coupling is typically weak; in contrast, coupling in acoustic systems can be easily manipulated by choices of materials and fabrication. Finally, the experimental realization of high-dimensional entangled elastic states will be of significant interest in quantum science as they can increase the available computing bandwidth for efficient quantum information processing. Therefore, this work lays the groundwork for quantum-like elastic physics and opens up avenues for information storage and processing modalities.

See the supplementary material for the details of the experimental materials and methods.

We acknowledge financial support from the W.M. Keck Foundation.

REFERENCES

1. F. Arute, K. Arya, R. Babbush, D. Bacon, J. C. Bardin, R. Barends, R. Biswas, S. Boixo, F. G. S. L. Brandao, D. A. Buell, B. Burkett, Y. Chen, Z. Chen, B. Chiaro, R. Collins, W. Courtney, A. Dunsworth, E. Farhi, B. Foxen, A. Fowler, C. Gidney, M. Giustina, R. Graff, K. Guerin, S. Habegger, M. P. Harrigan, M. J. Hartmann, A. Ho, M. Hoffmann, T. Huang, T. S. Humble, S. V. Isakov, E. Jeffrey, Z. Jiang, D. Kafri, K. Kechedzhi, J. Kelly, P. V. Klimov, S. Knysh, A. Korotkov, F. Kostritsa, D. Landhuis, M. Lindmark, E. Lucero, D. Lyakh, S. Mandrà, J. R. McClean, M. McEwen, A. Megrant, X. Mi, K. Michielsen, M. Mohseni, J. Mutus, O. Naaman, M. Neeley, C. Neill, M. Y. Niu, E. Ostby, A. Petukhov, J. C. Platt, C. Quintana, E. G. Rieffel, P. Roushan, N. C. Rubin, D. Sank, K. J. Satzinger, V. Smelyanskiy, K. J. Sung, M. D. Trevithick, A. Vainsencher, B. Villalonga, T. White, Z. J. Yao, P. Yeh, A. Zalcman, H. Neven, and J. M. Martinis, Nature **574**, 505 (2019).
2. P. Deymier and K. Runge, Crystals **6**, 44 (2016).
3. P. Deymier and K. Runge, *Sound Topology, Duality, Coherence and Wave-Mixing: An Introduction to the Emerging New Science of Sound* (Springer International Publishing, 2017).
4. L. Calderin, M. A. Hasan, N. G. Jenkins, T. Lata, P. Lucas, K. Runge, and P. A. Deymier, Sci. Rep. **9**, 14156 (2019).
5. M. Z. Hasan and C. L. Kane, Rev. Mod. Phys. **82**, 3045 (2010).
6. L.-H. Wu and X. Hu, Phys. Rev. Lett. **114**, 223901 (2015).
7. S. Yves, R. Fleury, T. Berthelot, M. Fink, F. Lemoult, and G. Lerosey, Nat. Commun. **8**, 16023 (2017).
8. P. Qiu, W. Qiu, J. Ren, Z. Lin, Z. Wang, J.-X. Wang, Q. Kan, and J.-Q. Pan, Nanoscale Res. Lett. **13**, 113 (2018).
9. Z. Zhang, Y. Tian, Y. Cheng, X. Liu, and J. Christensen, Phys. Rev. B **96**, 241306 (2017).
10. S. Yves, R. Fleury, F. Lemoult, M. Fink, and G. Lerosey, New J. Phys. **19**, 075003 (2017).
11. P. Wang, L. Lu, and K. Bertoldi, Phys. Rev. Lett. **115**, 104302 (2015).
12. S. H. Mousavi, A. B. Khanikaev, and Z. Wang, Nat Commun. **6**, 8682 (2015).
13. C. Brendel, V. Peano, O. Painter, and F. Marquardt, Phys. Rev. B **97**, 020102 (2018).
14. S.-Y. Yu, C. He, Z. Wang, F.-K. Liu, X.-C. Sun, Z. Li, H.-Z. Lu, M.-H. Lu, X.-P. Liu, and Y.-F. Chen, Nat. Commun. **9**, 3072 (2018).
15. Y. Long, J. Ren, and H. Chen, Proc. Natl. Acad. Sci. **115**, 9951 (2018).
16. R. Horodecki, P. Horodecki, M. Horodecki, and K. Horodecki, Rev. Mod. Phys. **81**, 865 (2009).
17. R. Raussendorf and H. J. Briegel, Phys. Rev. Lett. **86**, 5188 (2001).
18. S. Lloyd, Science **273**, 1073 (1996).
19. A. R. Calderbank and P. W. Shor, Phys. Rev. A **54**, 1098 (1996).
20. E. Knill, Nature **434**, 39 (2005).
21. T. Monz, P. Schindler, J. T. Barreiro, M. Chwalla, D. Nigg, W. A. Coish, M. Harlander, W. Hänsel, M. Hennrich, and R. Blatt, Phys. Rev. Lett. **106**, 130506 (2011).
22. X.-L. Wang, L.-K. Chen, W. Li, H.-L. Huang, C. Liu, C. Chen, Y.-H. Luo, Z.-E. Su, D. Wu, Z.-D. Li, H. Lu, Y. Hu, X. Jiang, C.-Z. Peng, L. Li, N.-L. Liu, Y.-A. Chen, C.-Y. Lu, and J.-W. Pan, Phys. Rev. Lett. **117**, 210502 (2016).
23. R. Barends, J. Kelly, A. Megrant, A. Veitia, D. Sank, E. Jeffrey, T. C. White, J. Mutus, A. G. Fowler, B. Campbell, Y. Chen, Z. Chen, B. Chiaro, A. Dunsworth, C. Neill, P. O'Malley, P. Roushan, A. Vainsencher, J. Wenner, A. N. Korotkov, A. N. Cleland, and J. M. Martinis, Nature **508**, 500 (2014).
24. L. F. Wei, Y. Liu, and F. Nori, Phys. Rev. Lett. **96**, 246803 (2006).
25. R. J. C. Spreeuw, Found. Phys. **28**, 361 (1998).
26. E. Karimi and R. W. Boyd, Science **350**, 1172 (2015).
27. P. Ghose and A. Mukherjee, Rev. Theor. Sci. **2**, 274 (2014).
28. C. E. R. Souza, J. A. O. Huguenin, P. Milman, and A. Z. Khoury, Phys. Rev. Lett. **99**, 160401 (2007).
29. L. Chen and W. She, J. Opt. Soc. Am., B **27**, A7 (2010).
30. C. V. S. Borges, M. Hor-Meyll, J. A. O. Huguenin, and A. Z. Khoury, Phys. Rev. A **82**, 033833 (2010).

[31]E. Karimi, J. Leach, S. Slussarenko, B. Piccirillo, L. Marrucci, L. Chen, W. She, S. Franke-Arnold, M. J. Padgett, and E. Santamato, Phys. Rev. A **82**, 022115 (2010).
[32]A. Vallés, V. D'Ambrosio, M. Hendrych, M. Mičuda, L. Marrucci, F. Sciarrino, and J. P. Torres, Phys. Rev. A **90**, 052326 (2014).
[33]L. J. Pereira, A. Z. Khoury, and K. Dechoum, Phys. Rev. A **90**, 053842 (2014).
[34]X.-F. Qian, B. Little, J. C. Howell, and J. H. Eberly, Optica **2**, 611 (2015).
[35]W. F. Balthazar, C. E. R. Souza, D. P. Caetano, E. F. Galvão, J. a O. Huguenin, and A. Z. Khoury, Opt. Lett. **41**, 5797 (2016).
[36]S. M. Hashemi Rafsanjani, M. Mirhosseini, O. S. Magaña-Loaiza, and R. W. Boyd, Phys. Rev. A **92**, 023827 (2015).
[37]P. A. Deymier, J. O. Vasseur, K. Runge, and P. Lucas, *Phonons in Low Dimensional Structures* (InTech Publisher, 2018).
[38]P. A. Deymier, K. Runge, J. O. Vasseur, A.-C. Hladky, and P. Lucas, J. Phys. B **51**, 135301 (2018).
[39]M. A. Hasan, L. Calderin, T. Lata, P. Lucas, K. Runge, and P. A. Deymier, Commun. Phys. **2**, 106 (2019).
[40]P. A. Deymier, K. Runge, M. A. Hasan, and L. Calderin, Materials **12**, 3553 (2019).
[41]C. Schmid, A. P. Flitney, W. Wieczorek, N. Kiesel, H. Weinfurter, and L. C. L. Hollenberg, New J. Phys. **12**, 063031 (2010).
[42]B. N. Simon, S. Simon, F. Gori, M. Santarsiero, R. Borghi, N. Mukunda, and R. Simon, Phys. Rev. Lett. **104**, 023901 (2010).
[43]A. R. C. Pinheiro, C. E. R. Souza, D. P. Caetano, J. a O. Huguenin, A. G. M. Schmidt, and A. Z. Khoury, J. Opt. Soc. Am., B **30**, 3210 (2013).
[44]A. B. Klimov, R. Guzmán, J. C. Retamal, and C. Saavedra, Phys. Rev. A **67**, 062313 (2003).
[45]M. Y. Niu, I. L. Chuang, and J. H. Shapiro, Phys. Rev. Lett. **120**, 160502 (2018).
[46]R. Das, A. Mitra, S. V. Kumar, and A. Kumar, Int. J. Quantum Inf. **1**, 387 (2003).
[47]D. M. Hugh and J. Twamley, New J. Phys. **7**, 174 (2005).
[48]Z. Gedik, I. A. Silva, B. Çakmak, G. Karpat, E. L. G. Vidoto, D. O. Soares-Pinto, E. R. deAzevedo, and F. F. Fanchini, Sci. Rep. **5**, 14671 (2015).
[49]M.-X. Luo, X.-B. Chen, Y.-X. Yang, and X. Wang, Sci. Rep. **4**, 1 (2015).
[50]B. P. Lanyon, M. Barbieri, M. P. Almeida, T. Jennewein, T. C. Ralph, K. J. Resch, G. J. Pryde, J. L. O'Brien, A. Gilchrist, and A. G. White, Nat. Phys. **5**, 134 (2009).
[51]D.-S. Wang, D. T. Stephen, and R. Raussendorf, Phys. Rev. A **95**, 032312 (2017).
[52]H.-H. Lu, J. M. Lukens, B. P. Williams, P. Imany, N. A. Peters, A. M. Weiner, and P. Lougovski, npj Quantum Inf. **5**, 24 (2019).
[53]X.-L. Wang, Y.-H. Luo, H.-L. Huang, M.-C. Chen, Z.-E. Su, C. Liu, C. Chen, W. Li, Y.-Q. Fang, X. Jiang, J. Zhang, L. Li, N.-L. Liu, C.-Y. Lu, and J.-W. Pan, Phys. Rev. Lett. **120**, 260502 (2018).
[54]M. Fiorentino and F. N. C. Wong, Phys. Rev. Lett. **93**, 070502 (2004).
[55]K. H. Kagalwala, G. Di Giuseppe, A. F. Abouraddy, and B. E. A. Saleh, Nat. Commun. **8**, 739 (2017).
[56]P. Imany, J. A. Jaramillo-Villegas, M. S. Alshaykh, J. M. Lukens, O. D. Odele, A. J. Moore, D. E. Leaird, M. Qi, and A. M. Weiner, npj Quantum Inf. **5**, 59 (2019).
[57]B. P. Lanyon, T. J. Weinhold, N. K. Langford, J. L. O'Brien, K. J. Resch, A. Gilchrist, and A. G. White, Phys. Rev. Lett. **100**, 060504 (2008).
[58]F. Dolde, V. Bergholm, Y. Wang, I. Jakobi, B. Naydenov, S. Pezzagna, J. Meijer, F. Jelezko, P. Neumann, T. Schulte-Herbrüggen, J. Biamonte, and J. Wrachtrup, Nat. Commun. **5**, 3371 (2014).
[59]Y. Maleki and A. M. Zheltikov, Phys. Rev. A **97**, 012312 (2018).
[60]Y. Maleki and A. M. Zheltikov, Opt. Express **26**, 17849 (2018).
[61]D. Janzing, in *Compendium of Quantum Physics*, edited by D. Greenberger, K. Hentschel, and F. Weinert (Springer, Berlin/Heidelberg, 2009), pp. 205–209.
[62]C. Gabriel, A. Aiello, W. Zhong, T. G. Euser, N. Y. Joly, P. Banzer, M. Förtsch, D. Elser, U. L. Andersen, C. Marquardt, P. S. J. Russell, and G. Leuchs, Phys. Rev. Lett. **106**, 060502 (2011).
[63]F. Töppel, A. Aiello, C. Marquardt, E. Giacobino, and G. Leuchs, New J. Phys. **16**, 073019 (2014).